Observation of laser transverse modes analogous to a SU(2) wave packet of a quantum harmonic oscillator

Y. F. Chen*
Department of Electrophysics, National Chiao Tung University, 1001 TA Hsueh Road, Hsinchu 30050, Taiwan, Republic of China

Y. P. Lan
Institute of Electro-Optical Engineering, National Chiao Tung University, Hsinchu, Taiwan, Republic of China

(Received 18 March 2002; revised manuscript received 22 July 2002; published 21 November 2002)

We report the generation of a new type of laser transverse mode that is analogous to a SU(2) elliptical wave packet of a quantum harmonic oscillator. Experimental results show that using a doughnut pump profile to excite an isotropic microchip laser in a spherical cavity can generate the elliptical transverse modes. The formation of elliptical transverse modes is found to be a spontaneous locking process of Hermite-Gaussian modes within the same family. The chaotic relaxation oscillation caused by the interaction of two nearly degenerate elliptical modes is also observed.

DOI: 10.1103/PhysRevA.66.053812 PACS number(s): 42.60.Jf, 42.55.Rz, 42.25.Kb, 42.50.Ar

I. INTRODUCTION

It is well known that the paraxial wave equation for the spherical laser resonators has the identical form with the Schrödinger equation for the two-dimensional (2D) harmonic oscillator [1]. The eigenfunction of the 2D quantum harmonic oscillator can be analytically expressed as Hermite-Gaussian function with Cartesian symmetry (x,y) or Laguerre-Gaussian function with cylindrical symmetry (r,ϕ) [2]. Since the functional forms of the 2D quantum oscillator and the spherical resonators are similar, the higher transverse modes of the spherical resonators can be in terms of the Hermite-Gaussian (HG) modes or the Laguerre-Gaussian (LG) modes. Recently, the pure high-order HG modes and LG modes have been successfully generated from a solid-state laser pumped with a fiber-coupled laser diode [3–5].

The quantum harmonic oscillator is an excellent pedagogical system to understand the basic properties of quantum mechanics, quantized radiation fields, quantum optics, and the concept of quantum-classical correspondence. Coherent states that were first proposed by Schrödinger in 1926 [6] have been shown to be very useful in the discussion of quantum-classical correspondence [7–9]. Recently, Pollet, Méplan, and Gignoux [10] demonstrated that the wave function of the SU(2) coherent state for the 2D quantum harmonic oscillation is particularly simple and well localized on the corresponding classical elliptical trajectory. Mathematically, the SU(2) coherent state is a superposition of the HG eigenstates with degenerate eigenvalue. Since output from a well stabilized laser is spontaneously a coherent state, it should be possible to observe the transverse modes within the corresponding SU(2) coherent states. So far, however, no experimental evidence exists for the observation of the elliptic SU(2) modes in laser resonators.

In this work we report the first observation of the lasing in the elliptic SU(2) modes in a microchip laser. It is found that generating elliptic SU(2) modes requires a large transverse-mode spacing as well as a nearly isotropic stimulated emission in the transverse plane. The experimental results also reveal that an infinitesimal imperfection in the symmetry leads to the elliptic modes near threshold to be the azimuthal standing waves not the azimuthal traveling waves. The formation of SU(2) coherent mode is found to be a spontaneous process of transverse-mode locking within degenerated mode families. Increasing the cavity Q factor, we observe the double-ring elliptical mode and the chaotic relaxation oscillation caused by the interaction of two nearly degenerate elliptical modes.

II. SU(2) COHERENT MODE

The HG eigenmode of the spherical resonator can be expressed as

$$E_{m,n}(x,y)=\frac{1}{\sqrt{2^{m+n-1}\pi m!n!}}\frac{1}{\omega_0}H_m\left(\frac{\sqrt{2}x}{\omega_0}\right)H_n\left(\frac{\sqrt{2}y}{\omega_0}\right)\times\exp\left[-\frac{(x^2+y^2)}{\omega_0^2}\right], \quad (1)$$

where ω_0 is the laser beam waist. The HG transverse mode can be equivalent to the wave function of the 2D quantum harmonic oscillator using the relationship

$$\omega_0^2=\frac{2\hbar}{m\omega}, \quad (2)$$

where m is the oscillator mass and ω is the angular frequency.

As in the Schwinger representation of the SU(2) algebra, SU(2) transverse-mode functions $\Psi_N(x,y)$ in the spherical resonators are formed by the superposition of the degenerate HG eigenmodes $E_{K,N-k}(x,y)$, where $K=0,1,2,...,N$,

*Corresponding author. FAX: (886-35) 729134. Email address: yfchen@cc.nctu.edu.tw

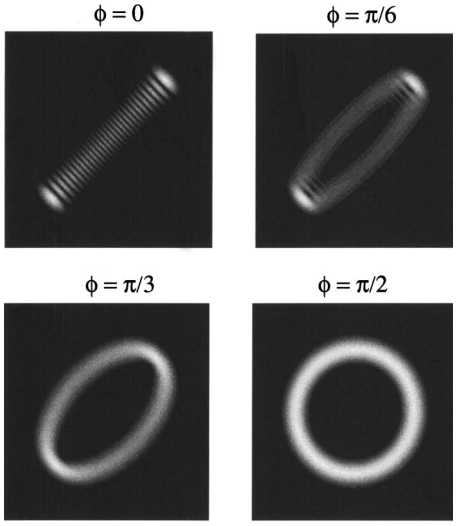

FIG. 1. The dependence of the SU(2) coherent mode on the phase φ of the parameter $\tau=\exp(i\varphi)$ for $N=30$.

$$\mathbf{\Psi}_N(x,y)=\frac{1}{(1+|\tau|^2)^{N/2}}\sum_{K=0}^{N}\binom{N}{K}^{1/2}\tau^K E_{K,N-k}(x,y). \quad (3)$$

The parameter τ is, in general, complex and $|\tau|^2$ is the ratio of the mean order of transverse modes in the x and y axes. In the limit $\tau\to 0$ (or $\tau\to\infty$), the SU(2) transverse-mode function becomes the eigenmode $E_{0,N}(x,y)$ [or $E_{N,0}(x,y)$]. For $|\tau|=1$, the mean order of transverse modes in the x and y axes is equal; therefore, the symmetrical axes of the SU(2) transverse pattern are along the diagonal $x=\pm y$. Using the addition formula, Eq. (3) can be expressed by the wave function

$$\mathbf{\Psi}_N(x,y)=\frac{1}{\sqrt{2^{N-1}\pi N!}}\left(\frac{1+\tau^2}{1+|\tau|^2}\right)^{N/2}\frac{1}{\omega_0}\times\exp\left[-\frac{(x^2+y^2)}{\omega_0^2}\right]H_N\left(\frac{\sqrt{2}(\tau x+y)}{\omega_0\sqrt{1+\tau^2}}\right). \quad (4)$$

The dependence of the transverse mode on the parameter τ can be figured out by using $\tau=\exp(i\varphi)$ and varying the phase φ from 0 to $\pi/2$, as shown in Fig. 1 for $N=30$. It is seen that the transverse patterns $|\mathbf{\Psi}_N(x,y)|^2$ for $\varphi=0$ and $\varphi=\pi/2$ are, respectively, the pure HG and LG modes at an angle $\pi/4$ with respect to the positive x axis. For $0<\varphi<\pi/2$, the transverse pattern displays coherent elliptic states at an angle $\pi/4$ with respect to the positive x axis. The elliptical stationary state illustrates geometrically Bohr's correspondence principle: the velocity of the classical particle is at a minimum at the two apogees of the motion, and therefore the transverse pattern has a peak at these points, as in the discussion of Ref. [9]. Recently, Allen *et al.* [11] showed that the orbital angular momentum per photon of an arbitrary normalized mode in the propagation direction (z direction) is equal to the expectation value $\langle L_z\rangle$, where the operator L_z takes the well-known form $-i\hbar(\partial/\partial\phi)$. With Eq. (1), the orbital angular momentum per photon of the SU(2) transverse mode with $\tau=\exp(\pm i\varphi)$ is found to be $\langle L_z\rangle=\mp N\hbar\sin\varphi$. This indicates that the generalized elliptic laser mode can have an average orbital angular momentum.

The elliptic states shown in Fig. 1 are the traveling waves in the azimuthal direction. Theoretical analysis for the laser transverse pattern formation indicates that an infinitesimal imperfection in the symmetry of the system may yield the standing waves in the azimuthal direction. The generalized standing wave is described by

$$\mathbf{\Phi}_N^{\pm}(x,y)=\frac{1}{\sqrt{2}}[\mathbf{\Psi}_N(x,y)\pm\mathbf{\Psi}_N^*(x,y)]. \quad (5)$$

Figure 2 depicts the typical transverse patterns for the SU(2) elliptical standing waves with $N=30$.

An important property of the $E_{m,n}$ modes is that their frequency depends on the indices m and n via the sum $m+n$. Equation (3) reveals that SU(2) transverse mode is a combination of HG modes of a frequency-degenerate family. The factor $\tau^k=\exp(ik\varphi)$ in Eq. (3) corresponds to an additional change of phase φ for each integer increase in the value of k. Since the special phase locking among the HG modes is needed, the formation of SU(2) elliptical mode generally requires the stimulated emission cross section to be transversely isotropic.

III. EXPERIMENTAL RESULTS AND DISCUSSION

More recently, the pure LG modes have been successfully generated by using a doughnut-shaped pump profile to pump an *a*-cut Nd:YVO_4 microchip laser. In the present experiment, we use a *c*-cut Nd:YVO_4 microchip laser to realize the generation of SU(2) elliptical mode. The YVO_4 crystal belongs to the group of oxide compounds crystallizing in a zircon structure with tetragonal space group. The fourfold symmetry axis is the crystallographic *c* axis. Perpendicular to this axis are the two indistinguishable *a* and *b* axes. The uniaxial Nd:YVO_4 crystal shows strong polarization-dependent fluorescence emission due to the anisotropic crystal field. In a Nd:YVO_4 crystal, for example, the stimulated emission cross section parallel to the *c* axis, $\sigma_{\parallel}=25\times10^{-19}$ cm^2, is four times higher than that orthogonal to the *c* axis, $\sigma_{\perp}=6.5\times10^{-19}$ cm^2, for the emission wavelength at 1064 nm [12]. A larger stimulated emission cross section, as usual, results in a lower pumping threshold for laser operation. Therefore, the conventional Nd:YVO_4 crystals are cut along the *a* axis, i.e., the so-called *a* cut, to use the stimulated emission cross section of $\sigma_{\parallel}$ to dominate the laser oscillation. However, the Nd:YVO_4 crystal should be cut along the *c* axis, i.e., the so-called *c* cut, to obtain an isotropic stimulated emission cross section in the transverse plane. This is the reason why we use the *c*-cut crystal instead of the *a*-cut crystal to implement the generation of the SU(2) elliptical mode.

The system schematic and the pump profile in the laser system are shown in Fig. 3. The experimental laser cavity that consists of one planar Nd:YVO_4 surface, high-reflection coated at 1064 nm and high-transmission coated at 809 nm for the pump light to enter the laser crystal, and a spherical

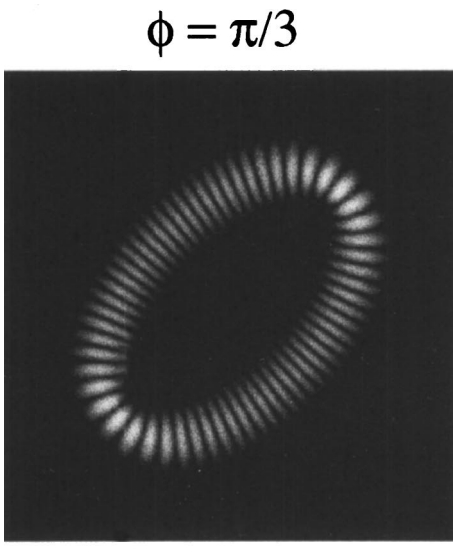

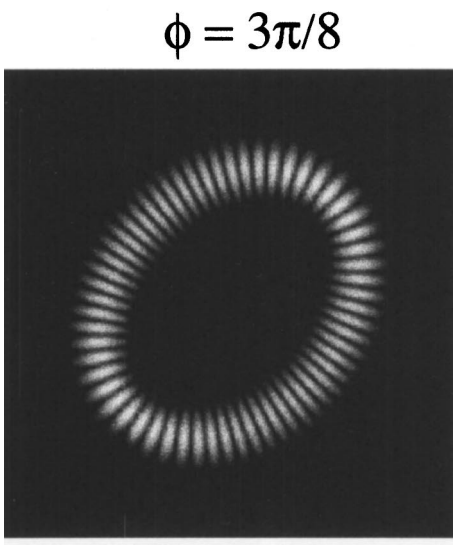

FIG. 2. The typical transverse patterns for the SU(2) elliptical standing waves with $N=30$.

output mirror is analogous to the one described in Ref. [5]. The gain medium in the experiment is *c* cut 2.0 at. % 1 mm length Nd:YVO_4 microchip crystal. The absorption coefficient of the Nd:YVO_4 crystal is about 6 mm^{-1} at 809 nm. We set up the resonator length to be as short as possible for reaching single-longitudinal mode operation. The total length in the present resonator is ~2.5 mm. The frequency spacing between consecutive longitudinal modes $\Delta\nu_L$ is about 60 GHz. The pump source is a 1-W fiber-coupled laser diode (Coherent, F-81-800C-100) with a 0.1-mm of core diameter. Note that the output intensity profile from an ordinary fiber-coupled laser diode is a top-hat distribution. The top-hat pump profile, as usual, leads to a complicated multitransverse HG mode without locking. With the special coupling condition, a fiber-coupled laser diode can have a doughnut output profile. Previously, we used the doughnut pump profile to successfully generate the pure LG mode. The present experimental results show that the SU(2) coherent modes

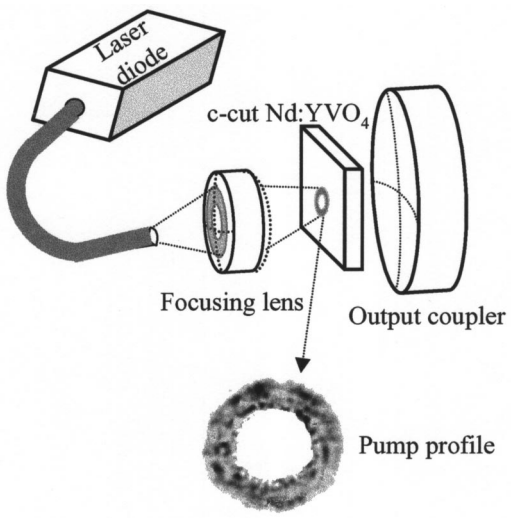

FIG. 3. Schematic of a fiber-coupled diode end-pumped laser; a typical pump profile of a fiber-coupled laser diode away from the focal plane.

cannot be generated without using the doughnut pump profile.

Since the SU(2) coherent modes are formed by the transverse HG mode families of frequency degenerate, the transverse-mode spacing $\Delta\nu_T$ plays a crucial role in the generation of the SU(2) elliptical modes. For the present cavity, the transverse-mode spacing is given by

$$\Delta\nu_T = \Delta\nu_L\left[\frac{1}{\pi}\cos^{-1}\left(1-\frac{L}{R}\right)^{1/2}\right], \tag{6}$$

where R is the radius of curvature of the output coupler. To investigate the influence of $\Delta\nu_T$ on the pattern, we use the output couplers with $R=250$, $R=50$, and $R=10$ mm in the present cavity. For $\Delta\nu_L=60$ GHz and $L=2.5$ mm, the transverse-mode spacing is found to be 1.9, 4.3, and 10 GHz, respectively, for $R=250$ mm, $R=50$ mm, and $R=10$ mm. Based on the thorough experiments, only the output coupler of $R=10$ mm can lead to the generation of the SU(2) elliptical coherent mode. In other cases, the output transverse pattern is a complex multitransverse HG mode without locking. The experimental data for the output coupler of $R=10$ mm will be presented hereafter.

First we used an output coupler with the reflectivity of 98% in the laser resonator. Near lasing threshold, the laser emits a pure high-order SU(2) elliptical coherent mode with the standing waves in the azimuthal direction. The order of the elliptical mode can be easily varied by controlling the pump size. The eccentricity of the lasing elliptical mode mainly depends on the spot size and incident angle of the pump beam. The measurement of the optical spectrum evidences that the elliptical mode is a single-frequency emission. In other words, the formation of the SU(2) elliptical mode can be interpreted as a spontaneous process of transverse-mode locking of the degenerate HG modes. Figure 4 shows two typical experimental results for the near-field transverse pattern on the concave mirror and the power

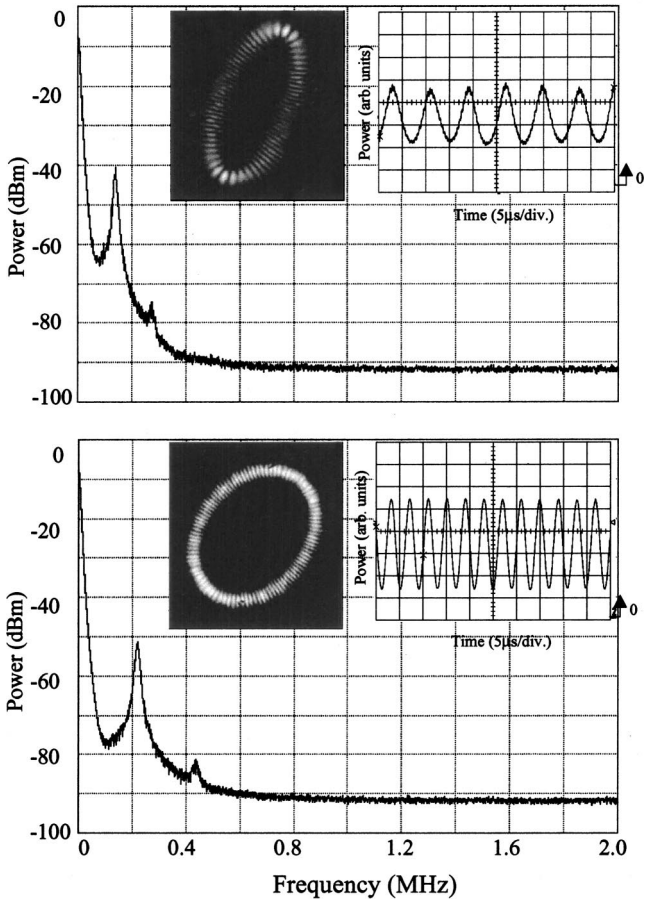

FIG. 4. Experimental results for the transverse patterns and power intensity spectra of two SU(2) elliptical standing waves near lasing threshold. The time traces are shown in the insets.

spectrum. The elliptical patterns are found to be preserved in free-space propagation. The preservation of the elliptical patterns consists of the property that HG modes remain HG filed patterns as they propagate. The power spectra of the free-running elliptical modes, as shown in Fig. 4, display relaxation oscillations. The behavior of the time trace is also shown in the inset of Fig. 4. In class-*B* lasers, relaxation oscillations arise from the energy coupling between field and inversion because the population inversion population acts as a mean flow. Therefore, the relaxation oscillation is the dynamic characteristics of the class-*B* laser in a single-mode operation. From the rate-equations analysis [13], the relaxation frequency is derived to be $f_r=\sqrt{2\gamma_{\|}\kappa(A-1)}/(2\pi)$, where κ and $\gamma_{\|}$ are, respectively, the decay constants of the electromagnetic field and of the population inversion, $A=P_{\mathrm{in}}/P_{\mathrm{th}}$ is the amount by which threshold is exceeded. Using the parameters for the present system ($\gamma_{\|}\approx 10^4\,\mathrm{sec}^{-1}$, $\kappa\approx 2.5\times 10^9\,\mathrm{sec}^{-1}$, and $A\approx 1.03\sim 1.05$), the relaxation frequency is calculated to be 0.19–0.25 MHz. The range of the calculated relaxation frequency is consistent with the experimental values shown in Fig. 4. Note that the relaxation oscillations play an important role in complex dynamics when the laser system is operated in multitransverse-mode emission or externally influenced (injection of external light, feedback, modulation of cavity losses).

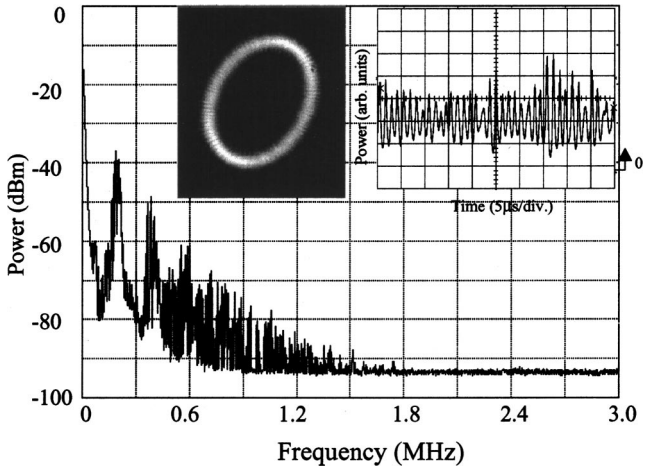

FIG. 5. Experimental results for the transverse patterns and power intensity spectra of the elliptical mode at 1.25 times above threshold. The time trace is shown in the inset.

Slightly above lasing threshold, a pair of elliptical modes $\mathbf{\Phi}_N^+(x,y)$ and $\mathbf{\Phi}_N^-(x,y)$ is simultaneously emitted with chaotic dynamics, as depicted in Fig. 5. Note that the elliptical modes $\mathbf{\Phi}_N^+(x,y)$ and $\mathbf{\Phi}_N^-(x,y)$ with the same longitudinal-mode index should be frequency degenerate without any perturbation. However, there is still a certain astigmatism in the present cavity because of thermal lensing effect in the gain medium. The appearance of dynamic chaos is believed to arise from the interaction of the relaxation frequency and the astigmatism-induced frequency difference between the elliptical modes $\mathbf{\Phi}_N^+(x,y)$ and $\mathbf{\Phi}_N^-(x,y)$. The time trace shown in Fig. 5 reveals that the signal-to-noise ratio is close to unity. A nonlinear system of the Maxwell-Bloch equations [5,14] was used to investigate the dynamics of two like modes in a class-*B* laser. It is found that there is a chaotic set of solutions when the astigmatism-induced frequency difference is close to the relaxation frequency. Note that the system of equations for the dynamics of a class-*B* laser operating in two like modes is similar to the system describing generation of counterpropagating wave in a bidirectional ring class-*B* laser, as discussed in Refs. [5,15,16]. Therefore, the condition for chaotic emission is also predicted in a bidirectional ring class-*B* laser [15].

The elliptical modes observed so far are linearly polarized along major axis. Increasing the reflectivity of the output coupler to 99%, we observed the appearance of the elliptical modes with the double ring, and the transverse patterns are linearly polarized along the orthogonal major and minor axes. Figure 6 depicts the polarization resolved patterns and the corresponding power spectra near lasing threshold. It can be seen that the transverse patterns of orthogonal polarizations have fundamentally different eccentricities. Although the two polarization modes are ideally degenerated in frequency, the thermally induced astigmatism may lift the degeneracy. Similar to the dynamics of two like modes in a class-*B* laser [5,14,17], chaos will appear when the frequency difference becomes of the order of the relaxation frequency. Since the corresponding patterns of different polarization are not degenerated in frequency, the total pattern in Fig. 6(a) is

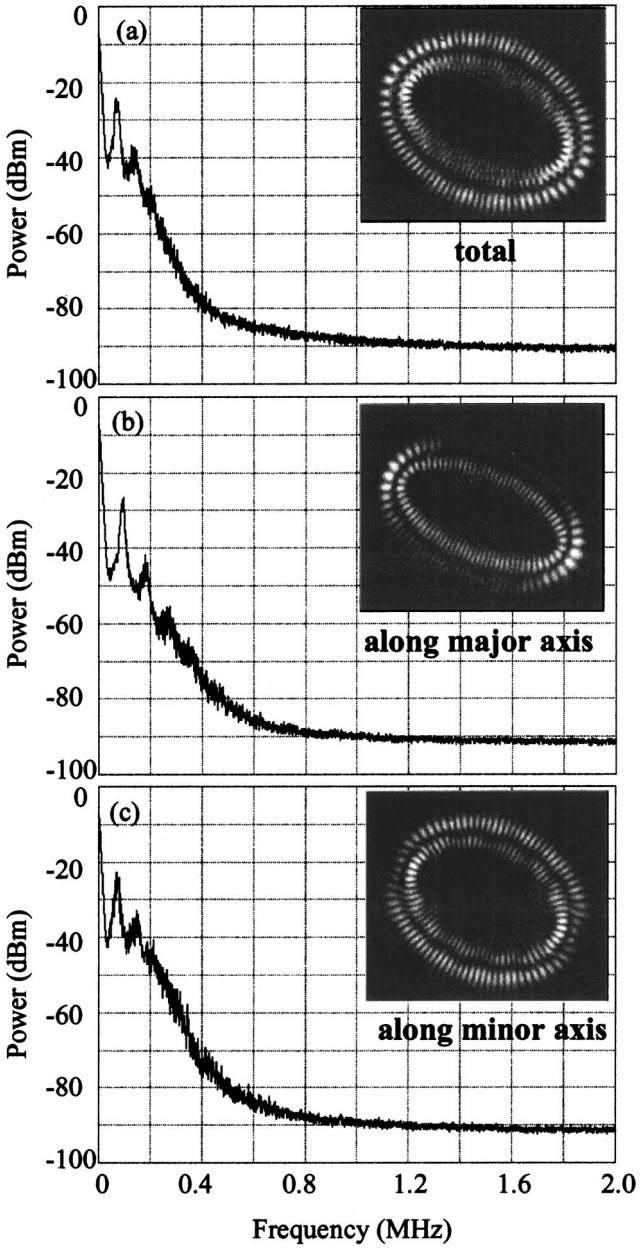

FIG. 6. Experimental results for the polarization resolved patterns and the corresponding power spectra near lasing threshold.

simply a superposition of the intensities in the orthogonal directions of polarization. As shown in Fig. 6, the broadening of the power spectra occurs in the total transverse pattern as well as the linearly polarized part. The typical behavior of the time trace is shown in Fig. 7. The large fluctuation in time trace indicates that the interaction between the two elliptical modes leads to the instability.

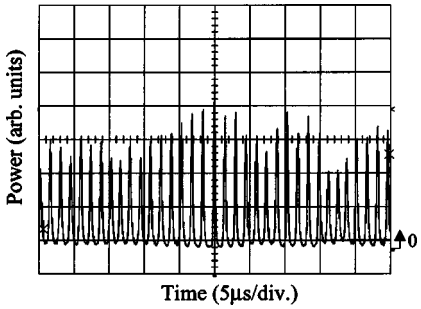

FIG. 7. The typical behavior of the time trace corresponding to the power spectrum shown in Fig. 6.

Finally, it is worthwhile to make a comparison between the present experiment and the experiment of Dingjan, van Exter, and Woerdman [18]. Both cases deal with off-axis pumping (a spot in the case of Ref. [18], a ring in the present case), and observe single-frequency emission of HG locked modes. The ratio of the transverse frequency spacing to longitudinal frequency spacing $\Delta\nu_T/\Delta\nu_L$ is 1/4 in case of Ref. [18]; however, it is 1/30 in the present case. The frequency locking in Ref. [18] occurs among different transverse orders with the help of different longitudinal orders, while here it occurs within the same family of transverse modes operating in a single-longitudinal mode. Self-organization, resulting from the frequency locking of two different families of transverse modes, has also been reported in a CO_2 laser [19].

IV. CONCLUSIONS

We have experimentally studied the formation of the SU(2) elliptical modes in a spherical cavity by using a doughnut pump profile to excite an isotropic microchip laser. The experimental results show that an infinitesimal imperfection in the symmetry leads to the elliptic modes near threshold to be the azimuthal standing waves. It is found that the formation of the SU(2) elliptical modes is a spontaneous process of transverse-mode locking within almost-degenerated mode families, and a large transverse-mode spacing is essential. Increasing the reflectivity of the output coupler, we observe the appearance of the double-ring elliptical mode and a chaotic relaxation oscillation.

ACKNOWLEDGMENT

The authors thank the National Science Council for their financial support of this research under Contract No. NSC-91-2112-M-009-030.

[1] H. Kogelnik and T. Li, Appl. Opt. **5**, 1550 (1966).
[2] S. Flügge, *Practical Quantum Mechanics* (Springer-Verlag, New York, 1971), p. 107.
[3] Y. F. Chen, T. M. Huang, C. F. Kao, C. L. Wang, and S. C. Wang, IEEE J. Quantum Electron. **33**, 1025 (1997).
[4] H. Laabs and B. Ozygus, Opt. Laser Technol. **28**, 213 (1996).
[5] Y. F. Chen and Y. P. Lan, Phys. Rev. A **63**, 063807 (2001).
[6] E. Schrödinger, Naturwissenschaften **14**, 644 (1926).
[7] F. Steiner, Physica B & C **151**, 323 (1988).
[8] W. M. Zhand, D. H. Feng, and R. Gilmore, Rev. Mod. Phys.

62, 867 (1990).
[9] R. F. Fox and M. H. Choi, Phys. Rev. A **61**, 032107 (2000).
[10] J. Pollet, O. Méplan, and C. Gignoux, J. Phys. A **28**, 7282 (1995).
[11] L. Allen, M. W. Beijersbergen, R. J. C. Spreeuw, and J. P. Woerdman, Phys. Rev. A **45**, 8185 (1992).
[12] H. Nagamoto, M. Nakatsuka, K. Naito, M. Yamanaka, K. Yoshida, T. Sasaki, T. Kanabe, A. Nakai, S. Saito, and Y. Kuwano, Laser Res. (in Japanese) **18**, 87 (1990).
[13] J. R. Tredicce, N. B. Abraham, G. P. Puccioni, and F. T. Arecchi, Opt. Commun. **55**, 131 (1985).
[14] D. V. Skryabin, A. G. Vladimirov, and A. M. Radin, Quantum Electron. **27**, 892 (1997).
[15] N. V. Kravtsov and E. G. Lariontsev, Quantum Electron. **24**, 841 (1994).
[16] A. G. Vladimirov, Opt. Commun. **149**, 67 (1998).
[17] K. Otsuka, S. L. Hwong, and B. A. Nguyen, Phys. Rev. A **61**, 053815 (2000).
[18] J. Dingjan, M. P. van Exter, and J. P. Woerdman, Opt. Commun. **188**, 345 (2001).
[19] E. Louvergneaux, G. Slekys, D. Dangoisse, and P. Glorieux, Phys. Rev. A **57**, 4899 (1998).